Small molecule activation at uranium coordination complexes: control of reactivity *via* molecular architecture

Ingrid Castro-Rodríguez[a] and Karsten Meyer†*[b]

Received (in Cambridge, UK) 27th September 2005, Accepted 15th November 2005
First published as an Advance Article on the web 24th January 2006
DOI: 10.1039/b513755c

Electron-rich uranium coordination complexes display a pronounced reactivity toward small molecules. In this Feature article, the exciting chemistry of trivalent uranium ions coordinated to classic Werner-type ligand environments is reviewed. Three fundamentally important reactions of the $[((^{R}ArO)_3tacn)U]$-system are presented that result in alkane coordination, CO/CO_2 activation, and nitrogen atom-transfer chemistry.

Introduction

From a synthetic chemist's perspective, it is rather remarkable that after fifty years of synthetic organometallic actinide research, much is still unknown about the non-aqueous inorganic coordination chemistry of low-valent uranium.[1,2]

[a]*Department of Chemistry, University of California, Latimer Hall, Berkeley, California, 94720, USA. E-mail: incasro@gmail.com; Tel: +1 510 642 2516*
[b]*Department of Chemistry and Biochemistry, University of California @ San Diego, 9500 Gilman Drive MC 0358, La Jolla, California, 92093-0358, USA*
† Present address: Friedrich-Alexander-University Nuremberg-Erlangen, Institute of Inorganic Chemistry, Egerlandstr. 1, 91058 Erlangen, Germany. E-mail: KMeyer@chemie.uni-erlangen.de, Fax: +49 (0)9131 8527367, Tel: +49 (0)9131 8527360

Historically, this is not surprising considering that until fairly recently, synthetic access to uranium(III) coordination compounds was restricted due to lack of suitable starting materials. With the exception of homoleptic $[(^{i\text{-}Pr}ArO)_3U]$[3] and its derivatives,[4] it was not until Clark and Sattelberger's synthesis of the solvated trivalent $[UI_3L_4]$ (L = THF and DME) and the solvent-free $[((Me_3Si)_2N)_3U]$[5] complexes reported in a 1997 issue of *Inorganic Synthesis* that coordination chemists finally had a synthetic protocol.[6–9] This provided a convenient and highly reproducible entry into the exciting world of trivalent uranium chemistry. In the literature of the following years, there is an increasing number of articles reporting classical inorganic coordination complexes of uranium, which employ traditional inorganic ligands such as

Ingrid Castro-Rodríguez

Ingrid Castro-Rodríguez was born in 1977 in Río Piedras, Puerto Rico. She received her Bachelor of Science degree in chemistry at the University of Puerto Rico (Río Piedras Campus) where she worked with Professor Reginald Morales on synthetic methods to isolate snake venoms. In fall 2000, Ingrid started her studies in the Department of Chemistry and Biochemistry at the University of California, San Diego, where she joined Karsten's laboratory in January 2001. Ingrid's research focused on the activation and functionalization of small molecules employing low-valent coordinatively unsaturated uranium complexes in sterically encumbering ligand environments. For her research accomplishments she received UCSD's Teddy Traylor award and a Carl Storm fellowship from the Gordon Research Conference. After receiving her PhD in inorganic chemistry in summer 2005, Ingrid was awarded a Glenn T. Seaborg postdoctoral fellowship and is currently working under the guidance of Professor Kenneth Raymond at the Lawrence Berkeley National Laboratory and University of California, Berkeley.

Karsten Meyer

Karsten Meyer was born in 1968 in Herne, Germany. In May 1995, he received his diploma in chemistry from the Ruhr-University Bochum. He then began his graduate education under the direction of Professor Karl Wieghardt at the Max-Planck-Institute for Bioinorganic Chemistry in Mülheim/Ruhr. Karsten's thesis work involved the synthesis and spectroscopic investigation of transition metal nitrido complexes. He received his doctoral degree in January 1998, which was awarded with distinction. Supported by a DFG postdoctoral fellowship, he continued his education by joining the laboratory of Professor Christopher C. Cummins at the Massachusetts Institute of Technology (Cambridge, MA) where he developed his passion for uranium chemistry. In January 2001 he was appointed to the faculty of the University of California, San Diego and was named an Alfred P. Sloan Fellow in summer 2004. Karsten has recently accepted a chair of inorganic chemistry at the University of Erlangen-Nuremberg where he will continue to pursue his research interests involving redox-active d-block and actinide metal complexes. The Meyer group specializes in manipulating complex reactivity by employing their understanding of molecular and electronic structure interplay.

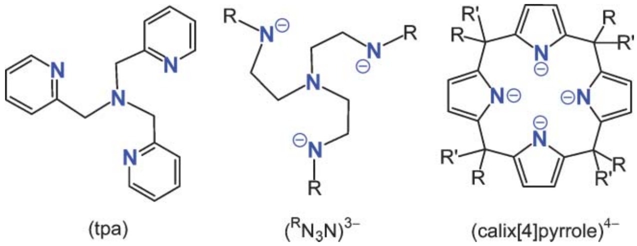

Chart 1 Selected chelating N-donor ligands for uranium coordination chemistry.

the chelating tris(2-pyridyl) and tris(2-pyrazinyl)methylamine (tpa and tpza),[10,11] hydro-tris(pyrazolyl)borate (Tp^-),[12] tris-(amido)amine ($^{R}N_3N^{3-}$),[13] macrocyclic calix[4]tetrapyrrole tetraanion[14] (Chart 1), as well as monodentate bis-(trimethylsilyl)amide and anilide ($Ar(R)N^-$) systems.[15]

The electron-rich trivalent complexes [$(N_3N)U$],[13] [(calix[4]pyrrole)U(dme)][K(dme)],[14] [$((Me_3Si)_2N)_3U$][9] and [$(N(R)Ar)_3U(THF)$][16] exhibit an unusual and interesting reactivity towards the activation of small inert molecules such as the first example of dinitrogen activation by an actinide compound. The reactivity of these new, more classical, coordination complexes exceeds, in some regards, that of the thoroughly explored archetypal [$(Cp)_3U$]-system and its derivatives.

The first example of dinitrogen fixation in actinide chemistry was reported by Scott and co-workers in 1998.[17] The trivalent uranium complex [$(N_3N)U$] (obtained *via* reduction of [$(N_3N)UCl$] and vacuum sublimation of the dinuclear precursor [$\{(N_3N)U\}_2(\mu\text{-Cl})$], where $N_3N = N(CH_2CH_2NSi\text{-}(t\text{-}Bu)Me_2)_3$) reversibly binds dinitrogen side-on forming the complex [$\{(N_3N)U\}_2(\mu{:}\eta^2,\eta^2\text{-}N_2)$] (Fig. 1). This uranium complex also reacts with trimethylsilyl azide and trimethylsilyl diazomethane to form the corresponding imido and hydrazido complexes.[13,18]

Shortly after the first diuranium dinitrogen complex was reported, Cummins and co-workers published the first stable heterodimetallic dinitrogen complex involving uranium.[16] The mononuclear trivalent [$(Ar(t\text{-}Bu)N)_3U(THF)$]·3THF complex, which by itself is unreactive towards N_2, was prepared employing the monodentate anilide ligand [$Ar(t\text{-}Bu)N^-$]. This trivalent uranium complex reacts with dinitrogen in the presence of the structurally very similar and exceedingly reactive [$(Ar(Ad)N)_3Mo$] to form the hetero-bimetallic bridged dinitrogen complex [$(Ar(Ad)N)_3Mo](\mu{:}\eta^1,\eta^1\text{-}N_2)[U(N(t\text{-}Bu)Ar)_3$] with an end-on coordinated N_2 ligand. It was suggested that this complex forms *via* nucleophilic attack of an intermediate molybdenum–dinitrogen complex [$(Ar(Ad)N)_3Mo(N_2)$] on the uranium(III) fragment.[16]

Another interesting reaction involving this class of compounds is the reaction of [$(Ar(R)N)_3U(I)$] ($R = C(CH_3)_3$, Ar = 3,5-$C_6H_3Me_2$) with toluene under strongly reducing conditions, which leads to the formation of [$\{(Ar(R)N)_2U\}_2(\mu\text{-}C_7H_8)$] (Fig. 2).[19,20] Following conventional electron-counting rules, the U centers in this dinuclear complex are assigned the formal oxidation state of +II. As expected for such a low-valent metal ion, this complex can be engaged in remarkable four-electron redox reactions with, *e.g.*, azobenzene and diphenyl disulfide compounds, yielding the uranium(IV/IV) species [$\{(N(R)Ar)_2U\}_2(\mu\text{-NPh})_2$] and [$\{(N(R)Ar)_2U(SPh)\}_2(\mu\text{-SPh})_2$], respectively.[19] However, the +II oxidation state has never been observed in U chemistry and thus, it was suggested that in this complex strong δ-back-bonding reduces and activates the bridging arene. The uranium center's ability to form strong covalent δ-bonds in the context of arene binding therefore provides access to a previously unknown divalent uranium synthon.

More recently, pyrrole-based polyanions have emerged as another class of versatile ligands for f-block metals. These supporting ligands have proven to substantially increase the reactivity of their low-valent metal complexes. This is especially evident for the chelation of trivalent uranium by the calix[4]tetrapyrrole tetraanion, which leads to binding and, most remarkably, cleavage of a dinitrogen ligand with formation of the unique μ-nitrido mixed-valent U^V/U^{IV} complex [$\{K(dme)(calix[4]tetrapyrrole)U\}_2(\mu\text{-NK})_2][K(dme)_4$] reported by Gambarotta in 2002.[21] The highly reactive uranium(III) complex was also shown to participate in solvent deoxygenation and polysilanol depolymerization processes.[21]

The above-mentioned discoveries by Scott, Cummins, Gambarotta and others have opened exciting new perspectives on actinide chemistry and evoked trust in the great potential offered by trivalent uranium complexes for unprecedented chemical transformations. Despite this increased interest in new modes of uranium reactivity, the coordination chemistry of uranium complexes with coordinated macrocyclic polyamine ligands remained largely unexplored. With the exception of

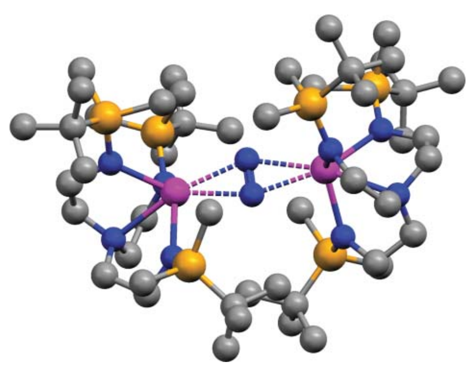

Fig. 1 X-Ray crystal structure of [$\{(N_3N)U\}_2(\mu{:}\eta^2,\eta^2)$] (CCDC code: PUKPEQ).

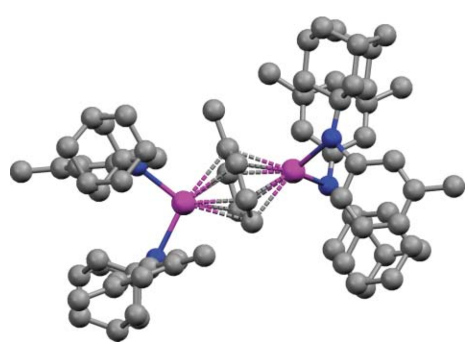

Fig. 2 Solid-state molecular structure of [$\{(Ar(Ad)N)_2U\}_2(\mu\text{-}C_7H_8)$] (CCDC code: QIZRUM).

our initial results in 2002[22] and an isolated report on a uranium complex of a tris-amido derivatized triazacyclononane in 2003 (Chart 2, right),[23] systematic studies on the molecular and electronic structure as well as the reactivity of uranium complexes supported by coordinated macrocyclic polyamine ligands[24] were missing from the literature. This is in contrast to the increasing amount of interesting data resulting from the thoroughly investigated organometallic chemistry of uranium with cyclopentadienyl ligands and their derivatives, as well as the more recently developed amido chemistry of uranium.

In our quest to identify and isolate uranium complexes with enhanced reactivity relevant to binding, activation, and functionalization of small molecules, we are currently investigating the coordination chemistry of uranium centers with classic Werner-type polyamine chelators. Our research was encouraged by the most recent exciting accomplishments in uranium coordination chemistry as outlined above, as well as by the well known benefits of macrocyclic chelators for stabilization of reactive transition metal ions.

This review presents the synthesis of complexes of uranium coordinated by polyamine macrocycle 1,4,7-tris(3,5-alkyl-2-hydroxybenzylate)-1,4,7-triazacyclononane.[25] Due to the small ring size of the neutral triazacyclononane macrocycle (tacn), this ligand by itself is obviously not a good chelator for the large hard uranium ion. Instead, the macrocyclic polyamine tacn was chosen to serve as an anchoring unit for stronger additional pendent arm ligands. This anchoring unit has proven to exhibit several distinct advantages for chelation of highly reactive uranium complexes. For instance, the polyamine ligand is a *weak* ligand for uranium ions, and consequently, the metal orbitals do not participate in strong metal–ligand interactions to the tacn fragment. Instead, the macrocycle is merely shielding one side of the ion while simultaneously serving as an anchor for strongly binding aryloxide pendant arms. As a result of the uranium ion's size and preference to bind hard ligands in a trigonal plane, aryloxides bind strongly to the central ion in a distorted trigonal planar fashion. This coordination geometry places aliphatic groups (R) *ortho* to the aryloxide in a manner that provides a protective cavity at the uranium ion's open and reactive coordination site. The molecular architecture of the axial binding site is greatly influenced by the alkyl-substituent R. Consequently, strategic choices of ligand substituents R

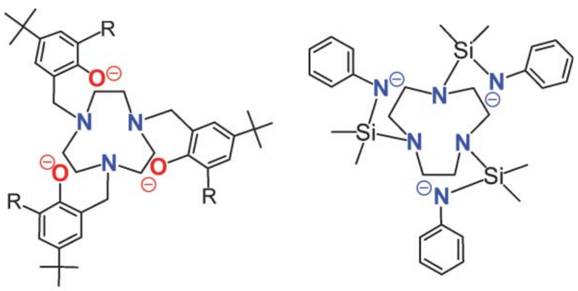

$(^{R}ArO)_3tacn^{3-}$ $(^{R}ArN)_3tacn^{3-}$

Chart 2 Tris-aryloxide (left) and tris-amido (right) triazacyclononane ligands for uranium coordination chemistry.

allow for control of complex reactivity *via* molecular architecture. Herein it is shown that electron-rich uranium complexes supported by an aryloxide-functionalized triazacyclononane ligand provide a unique platform for enhanced reactivity at a single uranium center. Specifically, we show that the introduction of hexadentate tris-anionic 1,4,7-tris(3,5-alkyl-2-hydroxybenzylate)-1,4,7-triazacyclononane derivatives ($(^{R}ArO)_3tacn^{3-}$ with R = *tert*-butyl (t-Bu)[25] and 1-adamantyl (Ad[26]) to redox-active uranium centers results in formation of stable, coordinatively unsaturated core complexes. This leaves a single axial coordination site (L) available for ligand binding, substitution reactions and redox events associated with small molecule activation and functionalization.

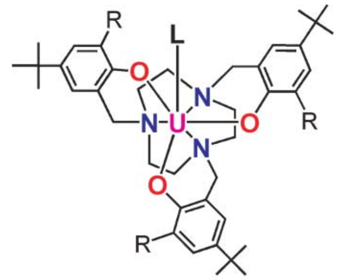

R = t-Bu	1	R = Ad	1-Ad
L = OAr	2	L = CO_2	7
μ–O	3	N_3	10
$NCCH_3$	4	$NSiMe_3$	11
μ–CO	5	NCO	12
μ–N_3	6	NCNMe	13
$NSiMe_3$	8	Cl	14
$NCPh_3$	8b	I	14b
NAd	8c		
N_3	9		

In addition, the unprecedented series of uranium III, IV, V, and VI complexes has provided a unique opportunity to study the electronic structure and bonding of analogous uranium complexes with identical core structures but differing formal oxidation states. A combination of synthetic, structural, spectroscopic (VT-VF SQUID magnetization, VT X-band EPR, UV/vis/NIR, and XANES spectroscopy), and computational investigations (DFT) of these complexes has provided fundamental insight into the nature and reactivity of the chemical bond in uranium coordination complexes.

1. Synthesis and characterization of low valent uranium(III) species and insights into their reactivity

1.1 Reactive uranium(III) precursor complexes of $(^{R}ArO)_3tacn^{3-}$

The first successful isolation of a mononuclear uranium-tacn complex was realized by treatment of the free 1,4,7-tris(3,5-di-*tert*-butyl-2-hydroxybenzyl)-1,4,7-triazacyclononane ($(^{t\text{-}Bu}ArOH)_3$-tacn)[25] with one equivalent of $[U(N(SiMe_3)_2)_3]$[8,9] in cold pentane solution. This protocol yields the six-coordinate uranium(III) complex $[((^{t\text{-}Bu}ArO)_3tacn)U]$ (**1**, Scheme 1) as a microcrystalline precipitate on a multigram scale.[22] The ^{1}H

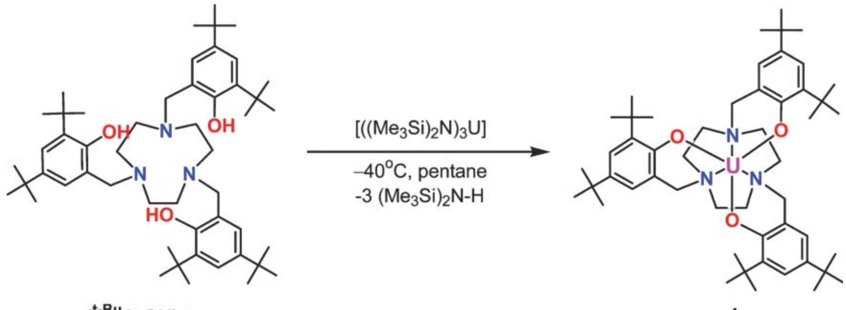

($^{t\text{-Bu}}$ArOH)$_3$tacn

1

Scheme 1 Scheme for synthesis of complex [(($^{t\text{-Bu}}$ArO)$_3$tacn)U] (**1**).

NMR spectrum of trivalent **1** (an f^3 species) recorded in benzene-d$_6$ at 20 °C displays ten paramagnetically shifted and broadened resonances between −22 and +13 ppm. The signal pattern is in agreement with an idealized C_3 symmetry, with the three pendent arms arranged in a twisted propeller-like arrangement. This splits the signals of the tacn backbone into four, and each methylene linkage into two diastereotopic hydrogens.[22]

Complex **1** can be prepared on a multi-gram scale, is stable in a dry N_2-atmosphere, and very soluble in hydrocarbon solvents. Yet, high quality single-crystals suitable for an X-ray diffraction study could not be obtained from pure solutions of pentane, hexane, benzene or toluene, nor mixtures thereof. Every attempt to re-crystallize **1** from ethereal solvents, such as Et_2O and THF at room or low temperature, yielded mono- and dinuclear seven-coordinate uranium(IV) complexes, namely [(($^{t\text{-Bu}}$ArO)$_3$tacn)U(OAr)] (**2**) and [{(($^{t\text{-Bu}}$ArO)$_3$-tacn)U}$_2$(μ-O)] (**3**).[22] Formation of **2** likely occurs *via* the sp^2–sp^3 bond cleavage by complex **1** on one of the methylene-linked phenolate pendent arms of the tris-aryloxide functionalized tacn ligand coordinated to another U(III) center. Similarly, dinuclear **3** forms almost quantitatively through C–O bond activation and oxygen atom abstraction of **1** from Et_2O and THF solvents. This observation demonstrates the underlying enhanced reactivity of monomeric, trivalent **1**. The solid-state molecular structures of **2** and **3** suggest that precursor complex **1** is indeed a six-coordinate mononuclear species with an unprotected and coordinatively unsaturated reactive site.

The X-ray diffraction analyses of single crystals of seven-coordinate **2** and **3** show an [N_3O_4]-ligand environment, with the fourth oxygen atom provided either by the η^1-bound aryloxide or a bridging oxo ligand, respectively. The average U–N(tacn) bond distances were determined to be 2.703 in **2** and 2.746 Å in **3**. The uranium–aryloxide interaction is strong, resulting in U–O(η^1-ArO) bond lengths of 2.195 Å ((ArO)$_3$tacn) and 2.165 Å (η^1-OAr) in **2** and 2.225 Å in **3**.[22] It will be shown below that the central uranium ion is displaced from an idealized plane formed by the three aryloxide oxygen atoms and toward the triazacyclononane macrocycle. Such as displacement is a distinct structural feature present in all complexes of this series. These out-of-plane shifts of the uranium centers in seven-coordinate **2** and **3** were determined to be −0.2 Å and −0.08 Å, respectively.

Careful recrystallization of **1** from acetonitrile at low-temperatures (−40 °C) yielded the purple crystalline compound [(($^{t\text{-Bu}}$ArO$_3$)tacn)U(NCCH$_3$)] (**4**).[27] The ^{1}H NMR spectrum of **4** in C_6D_6 is very similar to **1**, with resonances between −25 and 20 ppm. A resonance that could be unambiguously assigned to the acetonitrile methyl group was not observed. This can be attributed to the close proximity of the acetonitrile group to the paramagnetic U ion which broadens the acetonitrile signal to baseline levels. However, an X-ray diffraction study on single crystals of **4** revealed the axial acetonitrile molecule, completing the coordination sphere of the seven-coordinate trivalent uranium center. It is interesting to note that Cummins recently published a bimetallic radical cross coupling reaction of a benzonitrile adduct of the strongly reducing [(Ar(t-Bu)N)$_3$Mo] with a titanium(III) species in the presence of carbon dioxide.[28] The UV/vis and SQUID spectroscopic data of complex **4**, however, show that a reduction of the bound acetonitrile ligand in **4** does not occur and thus, a similar type of C–C bond or nitrile coupling was not observed for this complex. Similar to the coordination polyhedron of **2** and **3**, **4** can be described as distorted trigonal prismatic with an off-centered uranium ion shifted toward the trigonal plane formed by the three aryloxide oxygen atoms. The average U–O, U–N(CH_3CN), and U–N(tacn) bond distances were determined to be 2.26 Å, 2.66 Å, and 2.70 Å, respectively.[27]

The out of plane shift of the U ion with respect to the tris-aryloxide plane was determined to be −0.442 Å below the trigonal plane, deviating significantly from the displacement of the uranium(IV) ion in the tetravalent complexes **2** and **3**. It therefore appears that this structural parameter varies significantly with the strength (covalency) of the axial ligand and the uranium ion's oxidation state.

Considering the weak tacn-coordination and the metal ion's position with respect to the hard aryloxide ligands, the coordination geometries in complexes **1–4** might actually be considered trigonal (**1**) or trigonal-pyramidal (**2–4**), and therefore are similar to structures of the four-coordinate tris-aryloxide,[3] trimethylsilyl amido[9] and anilide systems.[16] The macrocyclic tacn chelator merely serves as an anchor for the potent aryloxide ligators, while also providing efficient protection of the U ion's ''backside''.

1.2 Metal–alkane coordination

Aware of the enhanced reactivity of trivalent [($^{t\text{-Bu}}$ArO)$_3$-tacn)U] (**1**) towards ''non-innocent'' solvents, we decided to

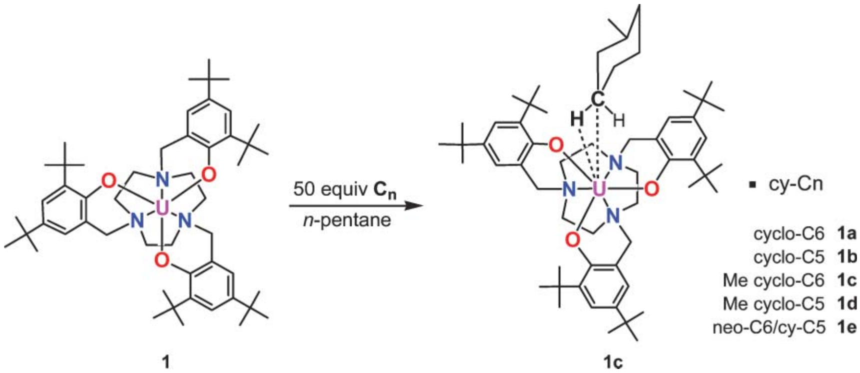

Scheme 2 Synthesis of $[((^{t\text{-}Bu}ArO)_3tacn)U(alkane)]\cdot(cycloalkane)$.

challenge its reactivity and expose the complex to more inert solvents like alkanes. Remarkably, recrystallization of **1** from pentane solutions containing various cycloalkanes, *i.e.* cyclohexane, afforded the coordination of one cycloalkane molecule to the electron-rich U center (Scheme 2).[29]

The X-ray diffraction analysis of these complexes (**1a–1e**) revealed atom positions and connectivities of one molecule of alkane in the coordination sphere of the uranium(III) center and a second molecule of cycloalkane co-crystallized in the lattice. Molecules **1a–1e** are isostructural, isomorphous, and all crystallize in the monoclinic space group $P2_1/n$. Fig. 3 shows the molecular structure of **1c** representative of the series of uranium–alkane complexes. The U–O(ArO) and U–N(CH_3CN) core structural parameters of all alkane-adducts **1a–1e** vary from 2.24 to 2.26 and 2.67 to 2.69 Å, respectively,[29] and thus, are similar to those found for the previously characterized acetonitrile adduct **4** and slightly shorter than those found in tetravalent **2** and **3**.

Most interestingly, the U–carbon bond distances to the axial cycloalkane *d*(U–C1S) in **1c** and **1d** were determined to be 3.864 and 3.798 Å, with the shortest U–carbon bond distance of 3.731 Å found in the solid-state structure of complex **1e**. Considering that the sum of the van der Waals radii for a U–CH_2 or U–CH_3 contact is 3.9 Å,[30–32] the shorter U–C distances found in complexes of **1a** to **1e** are indicative of a weak but significant orbital interaction. Upon closer inspection, the structures of **1a–1e** exhibit short contacts between the peripheral *tert*-butyl groups and the axial alkane ligand (2.12 and 2.71 Å), thus, the observed alkane coordination may be additionally supported by van der Waals interactions. X-ray diffraction analysis of complexes **1c–1e** allows for calculation of the hydrogen atoms in proximity to the uranium center (calculated positions; *d*(C–H) = 0.96 Å). For all structures, an η^2-H,C coordination mode is observed that seems to be favored for the metal–alkane binding.[29]

In agreement with the observed dependence of the uranium ion's out-of-plane shift with varying U oxidation state and ligand strength, the uranium displacement in trivalent complexes **1c–1e** with exceedingly weakly interacting alkanes were determined to be −0.66 Å below the aryloxide plane (compared to −0.44 Å in seven-coordinate **4**).

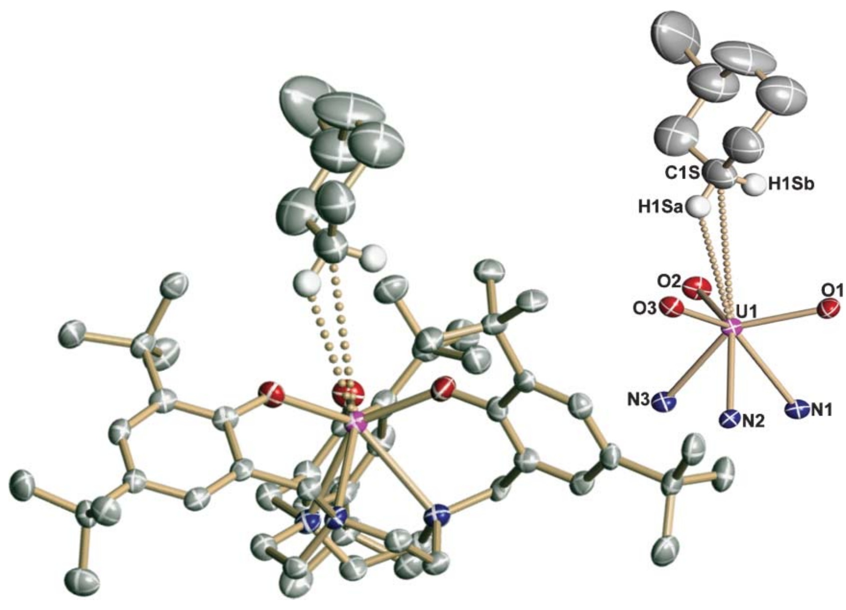

Fig. 3 Molecular representation of $[((^{t\text{-}Bu}ArO)_3tacn)U(^{Me}cy\text{-}C6)]$, (**1c**). The dotted lines emphasize the η^2-H,C alkane coordination.

2. C1 coordination and activation chemistry

Due to the vastness of its supply, the greenhouse gas CO_2 represents a valuable and renewable C1 source for the production of fine chemicals and fuels. Therefore, the interest in metal-mediated multi-electron reduction of carbon dioxide remains high. The continued interest in uranium carbonyl coordination is documented by the $[(Cp)_3U(CO)]$ success story. First synthesized in 1986 by Andersen *et al.*, $[(Cp)_3U(CO)]$[33] derivatives of the parent system were crystallographically characterized in 1995[34] and 2003.[35] Encouraged by the remarkable reactivity of our complexes, we set out to exploit this reactivity for CO_2 and CO activation and reduction.

2.1 Carbon monoxide activation assisted by $[((^{t\text{-}Bu}ArO)_3tacn)U]$

A pentane solution of coordinatively unsaturated, trivalent **1** cleanly reacts with carbon monoxide by binding and activating the CO, resulting in rapid and quantitative formation of μ-CO bridged diuranium species $[\{((^{t\text{-}Bu}ArO)_3tacn)U\}_2(\mu\text{-}CO)]$ (**5**, Scheme 3).[36] Infra-red vibrational spectra of this material reproducibly show a band at 2092 cm^{-1} (in Nujol) suggestive of a CO ligand. However, this frequency appears to be rather high for a coordinated and activated CO molecule. Despite numerous attempts, CO isotopomers of **5** could not be synthesized. This puzzling lack of success in isotopomer synthesis is likely due to impurities in commercially available sources of CO isotopes that, among other impurities, contain up to 20 ppm CO_2 and O_2. Both impurities lead to rapid formation of μ-oxo bridged **3**, the only isolable product of all labeling attempts (see below). To circumvent this problem, *in situ* generation of ^{13}CO will be attempted in the near future.

The molecular structure of **5** was characterized crystallographically and revealed an iso-carbonyl bonding motif, which is unique in actinide chemistry.[36] A representative structure $[\{((^{t\text{-}Bu}ArO)_3tacn)U\}_2(\mu\text{-}CO)]$ in crystals of $\mathbf{5}\cdot 3C_6H_6$, (Fig. 4) was modeled by employing an asymmetrical U–CO–U entity, with one short U–C bond and a longer U–O isocarbonyl interaction, disordered on two positions at the inversion center (rhombohedral space group R_3). The molecular structure of **5** exhibits two staggered $[((^{t\text{-}Bu}ArO)_3tacn)U]$-fragments linked *via* a linearly bridged CO ligand in a $\mu{:}\eta^1,\eta^1$ fashion. The resolution of the data is limited and, therefore, no reliable bond distances between the CO ligand and the U center can be provided. Considering the unusual frequency of the ν(CO) stretch and the crystallographic disorder, it should be emphasized that the corresponding dinitrogen-bridged species could not be synthesized, neither under ~1 atm nor an overpressure (80 psi) of N_2 gas, rendering the assignment of the disordered bridging CO-atoms unambiguous.

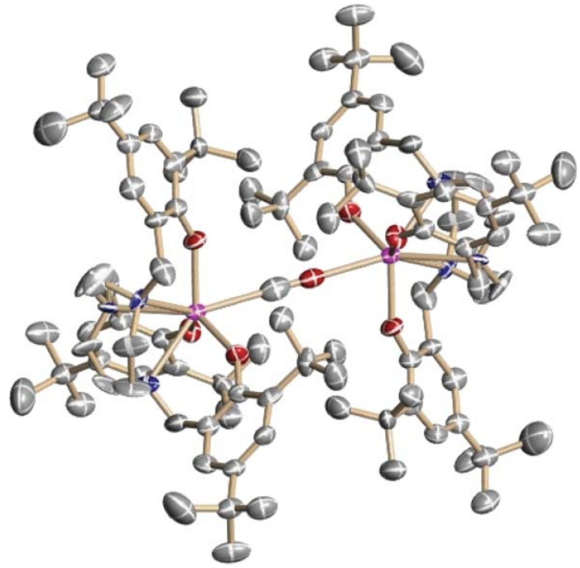

Fig. 4 Molecular representation of $[\{((^{t\text{-}Bu}ArO)_3tacn)U\}_2(\mu\text{-}CO)]$ (**5**).

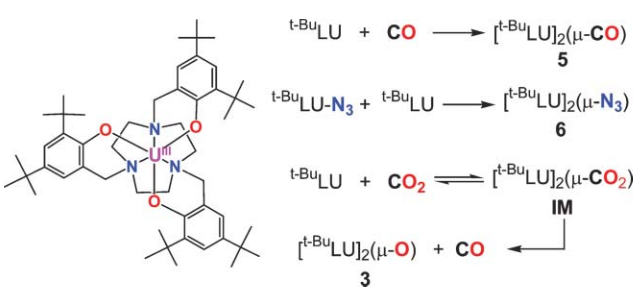

Scheme 3 Synthesis of $[\{((^{t\text{-}Bu}ArO)_3tacn)U\}_2(\mu\text{-}O)]$ (**3**), $[\{((^{t\text{-}Bu}ArO)_3tacn)U\}_2(\mu\text{-}CO)]$ (**5**), and $[((^{t\text{-}Bu}ArO)_3tacn)U(\mu\text{-}N_3)]$ (**6**).

The U–O(ArO) and U–N(tacn) distances in **5** were determined to be 2.185(5) and 2.676(4) Å. This U–N(tacn) bond distance is very similar to that found in the $[((^{t\text{-}Bu}ArO)_3tacn)U]$ fragments of $[((^{t\text{-}Bu}ArO)_3tacn)U(alkane)]$ (d(U–N(tacn)) = 2.676(6) Å)[29] and $[((^{t\text{-}Bu}ArO)_3tacn)U(NCCH_3)]$ (d(U–N(tacn)) = 2.699(6) Å).[27] In contrast, the average U-O(ArO) bond distance in **5** is significantly shorter than those found in structurally related trivalent $[((^{t\text{-}Bu}ArO)_3tacn)U]$ complexes.

The displacement of the uranium ion out of the idealized trigonal aryloxide plane towards the coordinated triazacyclononane polyamine chelator in **5** was determined to be only −0.377 Å. A diagram delineating this structural parameter for known complexes of the $[((^{t\text{-}Bu}ArO)_3tacn)U(L_{ax})]$ type clearly illustrates a linear correlation of higher oxidation states with smaller out-of-plane shifts (Fig. 5).[27,36,37] Based on this

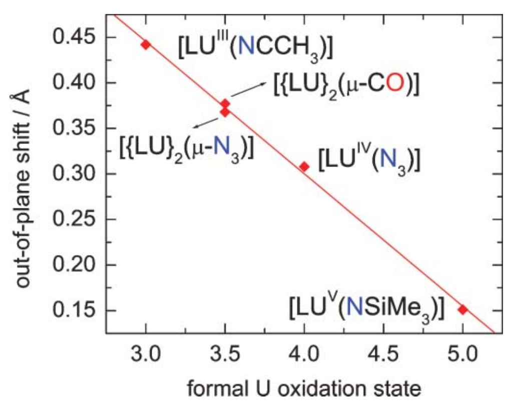

Fig. 5 Plot of the uranium ion's out-of-plane shift *vs.* the formal U oxidation state (see section 3 for $[((^{t\text{-}Bu}ArO)_3tacn)U(L_{ax})]$ with L_{ax} = N_3^- and Me_3SiN^{2-}).

correlation and in agreement with the crystallographic disorder, **5** can be assigned an average oxidation state of +3.5, suggestive of a mixed-valent uranium(III/IV) species. We suggested that **5** forms *via* a charge-separated U(IV)–$CO^{\bullet -}$ intermediate, which reacts with excess **1** to yield the formally mixed-valent U(IV)–CO–U(III) species **5**.

In this context, the μ-azido-bridged U(III/IV) species $[\{(L)U\}_2(\mu\text{-}N_3)]$ (**6**) was synthesized by reacting $[(L)U^{IV}(N_3)]$ with $[LU^{III}]$ to serve as an isostructural (and isomorphous, rhombohedral space group R_3) analogue of triatomic-bridged intermediate **IM** (see below) as well as an electronic model for mixed-valent **5** (Scheme 3). The out-of-plane shift found in mixed-valent **6** (−0.368 Å) is virtually identical to **5** (Fig. 5) and thus supports the charge-separation proposed for mixed-valent **5**.

2.2 Carbon dioxide coordination and activation assisted by $[((^{R}ArO)_3tacn)U]$

Addition of CO_2-saturated pentane to the deeply colored solution of red-brown **1** in pentane affords a colorless solution and subsequent formation of a pale-blue solution and CO-gas. The pale-blue material was identified as the known μ-oxo bridged diuranium(IV/IV) complex $[\{((^{t\text{-}Bu}ArO)_3tacn)U\}_2(\mu\text{-}O)]$ (**3**, see above).[36] The driving force for this remarkable $2e^-$ cleavage reaction of the thermodynamically stable CO_2 molecule likely is the concerted two-ion U(III) to U(IV) oxidation, the most stable oxidation state in this system. Additionally, this reaction is sterically facilitated by the ligand environment. Attempts to isolate this colorless intermediate *via* solvent evaporation in vacuum resulted in recovery of **1** (Scheme 3). We suggest a dinuclear CO_2-bridged diuranium species **IM** as a possible intermediate. The reaction of **1** with CO_2 is reminiscent of the reductive cleavage of COS by $[(Cp')_3U]$ ($Cp' = MeC_5H_4$), proceeding *via* a COS-bridged intermediate.[38,39] Accordingly, complete $2e^-$ reduction of CO_2 to yield CO and **3** likely proceeds stepwise *via* a fleeting CO_2-bridged intermediate, colorless **IM**, that is in equilibrium with **1** and CO_2.

After consideration of the dimerization products formed by complex **1**, it seemed likely that the *tert*-butyl derivatized ligand employed did not provide sufficient steric bulk to obstruct a complete $2e^-$ reduction of CO_2 to CO. In order to further study this unique CO_2 activation at the electron-rich uranium center, a ligand was needed that could provide greater steric bulk and allow for better protection of the open uranium coordination site. This steric bulk was provided in the next generation of our aryloxide-functionalized ligand system and the corresponding uranium complex, $[((^{Ad}ArO)_3tacn)U]$ (**1-Ad**).

2.3 The need for a sterically more demanding ligand

Our initial results on the *tert*-butyl derivatized $[((^{t\text{-}Bu}ArO)_3tacn)U]$-system have suggested that undesired side-reactions *trans* to the reactive site are effectively eliminated due to shielding by the triazacyclononane fragment. However, it is also evident that the *ortho*-functionalized *tert*-butyl groups of the three aryloxide pendant arms do not form a protective cavity at the reactive, electron-rich uranium center. Instead, the tilted aryloxides force the *tert*-butyl groups to form a bowl-shaped cavity (Fig. 6) with little protection to prevent decomposition reactions, such as ligand and solvent degradation as well as formation of dinuclear complexes. It seemed clear that if reactive intermediates could be better protected, a uranium(III) complex of the general $[((ArO)_3tacn)U]$-type would provide a powerful platform for reactivity studies at the apical position. In order to prevent dimerization, a sterically more encumbering derivative was required. Accordingly, protocols for the synthesis of the adamantane-functionalized ligand 1,4,7-tris(3-adamantyl-5-*tert*-butyl-2-hydroxybenzyl)1,4,7-triazacyclononane, $(^{Ad}ArOH)_3tacn$, and its corresponding U(III) precursor complex $[((^{Ad}ArO)_3tacn)U]$ (**1-Ad**) were developed.[26]

Similar to the preparation of **1**, reaction of $(^{Ad}ArOH)_3tacn$ with one equivalent of $[U(N(SiMe_3)_2)_3]$ in benzene yielded the six-coordinate U(III) complex $[((^{Ad}ArO)_3tacn)U]$ (**1-Ad**) as a red-brown powder in multigram quantities.[26] In striking contrast to **1**, complex **1-Ad** is stable in chlorinated and ethereal solutions and thus can be re-crystallized from mixtures of Et_2O/CH_2Cl_2. Single-crystals of **1-Ad** were studied by X-ray crystallography[26] and its molecular core structure was compared to its parent complex as found in $[((^{t\text{-}Bu}ArO)_3tacn)U(^{Me}cy\text{-}C6)]$ (**1c**, bound alkane omitted for clarity).[29]

A comparison of the core molecular structures in **1** and **1-Ad** show comparable U–O(ArO) and U–N(tacn) bond distances (see Table 1). The most striking difference in these structures is the displacement of the U ion from the trigonal aryloxide plane. While the out-of-plane shift in **1** is −0.66 Å, the uranium ion in **1-Ad** was found to be −0.88 Å below the aryloxide plane. The U ion displacement from the aryloxide

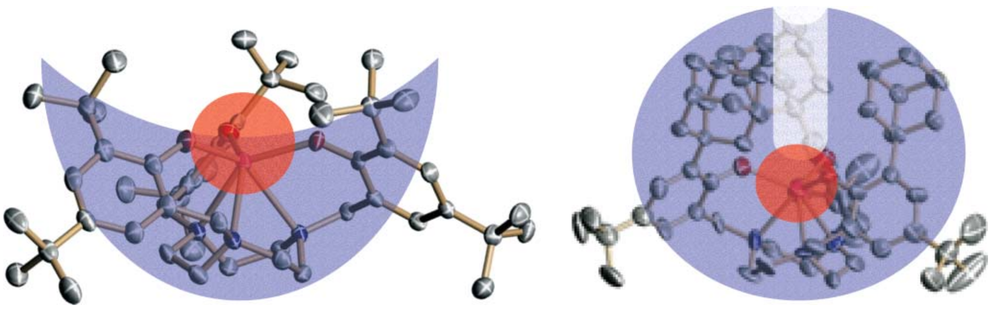

Fig. 6 Molecular structures and schematic representation of steric characteristics in $[((^{t\text{-}Bu}ArO)_3tacn)U]$ (**1c**, left) and $[((^{Ad}ArO)_3tacn)U]$ (**1-Ad**, right).

Table 1 Selected core structural parameters for complexes [((${}^{t\text{-}Bu}$ArO)$_3$-tacn)U] (**1c**) and [((^{Ad}ArO)$_3$tacn)U] (**1-Ad**, two independent molecules)

Structural parameters/Å	**1c**	**1-Ad**
d(U–N1$_{tacn}$)	2.656(4)	2.633(9)/2.648(8)
d(U–N2$_{tacn}$)	2.679(4)	2.609(10)/2.669(10)
d(U–N3$_{tacn}$)	2.692(4)	2.677(11)/2.628(10)
d(U–N$_{av}$)	2.68	2.64
d(U–O1$_{ArO}$)	2.261(3)	2.214(10)/2.219(8)
d(U–O2$_{ArO}$)	2.251(3)	2.218(9)/2.220(9)
d(U–O3$_{ArO}$)	2.220(3)	2.239(9)/2.248(8)
d(U–O$_{av}$)	2.24	2.23
U$_{out\text{-}of\text{-}plane\ shift}$	−0.66	−0.85

plane in addition to the increased steric bulk provided by the adamantane substituents of **1-Ad** lead to a narrow and approximately 4.7 Å deep cylindrical cavity. This cavity provides restricted access of an incoming ligand to the uranium ion, thereby protecting the uranium center from bimolecular decomposition reactions (Fig. 6).

Accordingly, exposure of intensely colored [((^{Ad}ArO)$_3$tacn)U] (**1-Ad**) in toluene or solid-state to CO_2 gas (1 atm) results in instantaneous discoloration of the samples.[37] Colorless crystals of [((^{Ad}ArO)$_3$tacn)U(CO_2)] (**7**) can be isolated from a saturated CH_2Cl_2/Et_2O solution. The infrared spectrum in nujol exhibits a distinct vibrational band centered at 2188 cm^{-1}, indicative of a coordinated and activated CO_2 ligand. The ^{12}C/^{13}C isotopic ratio R(2188/2128) of 1.0282 is close to that of free CO_2 gas (R 2349/2284 = 1.0284), suggestive of a molecule that has the same linear geometry as that of free CO_2 as well as the same carbon motion in the v_3 (v_{as}(OCO)) vibrational mode. While the assignment of this vibrational band is unambiguous, we note that the v_{as}(OCO) found in **7** is significantly higher than frequencies observed for other mononuclear M–CO_2 complexes with carbon- (η^1-**C**O$_2$) and carbon–oxygen-bound (η^2-**OC**O) bent CO_2 ligands, in which v_{as}(OCO) were reportedly found between 1550 and 1750 cm^{-1} (Scheme 4).[40]

In mononuclear complexes, such as Aresta's archetypal [(Cy$_3$P)$_2$Ni(CO_2)] (Cy = cyclohexyl)[41,42] and Herskowitz's [(diars)$_2$M(CO_2)(Cl)] (diars = *o*-phenylene bis(dimethylarsine); M = Ir, Rh),[43] the CO_2 ligand is coordinated in a bent η^1-**C**O$_2$ or η^2-**OC**O fashion, the only previously known coordination modes for M–CO_2 complexes. Among the few structurally characterized M–CO_2 complexes,[40] only [(Cy$_3$P)$_2$Ni(CO_2)][44] and [(bpy)$_2$Ru(CO_2)(CO)][45] are shown here for illustrative purposes (Fig. 7).

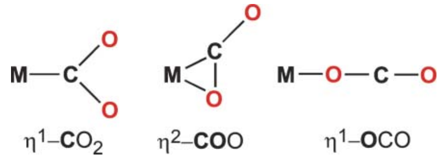

Scheme 4 Coordination modes in mononuclear M–CO_2 complexes.

It should be mentioned that the linear metal–CO_2 coordination mode has been implicated in biological processes such as photosynthesis and previously had been suggested for the crystal structure of the iron-containing enzyme α-ketoglutarate reductase.[46] Therefore it appears likely that end-on O-coordination is critical for binding, activation, and, most importantly, C-functionalization of the bound CO_2 molecule.

An X-ray diffraction analysis of the colorless single-crystals obtained from the reaction of **1-Ad** with CO_2 confirmed the presence of such a linearly coordinated and, more importantly, significantly activated CO_2 ligand. The CO_2 ligand in [((^{Ad}ArO)$_3$tacn)U(CO_2)]·2.5Et_2O (**7**·2.5Et_2O) is coordinated to the U ion in a never before structurally characterized, yet often speculated about, linear oxygen-bound η^1-**O**CO fashion (Fig. 8).[40] This CO_2 coordination mode was previously unprecedented in synthetic coordination chemistry and is likely enforced by the adamantyl substituents of the supporting ligand platform. The U–OCO group has a U–O bond length of 2.351(3) Å; the neighboring C–O bond length is 1.122(4) Å, and the terminal C–O bond length is 1.277(4) Å. The U–O–C and O–C–O angles of 171.1(2)° and 178.0(3)°, respectively, are close to linear.

These metric parameters, together with the red-shifted frequency of the vibrational bands (v_3:v_{OCO} = 2188 cm^{-1}, v_{OCO} = 2128 cm^{-1}), strongly suggest a molecular structure with charge-separated resonance structures U(IV)=O=C$^•$–O$^-$ ↔ U(III)–$^+$O≡C–O$^-$. The U(III) ion is either coordinated to a charge-separated CO_2 ligand or oxidized and the CO_2 ligand

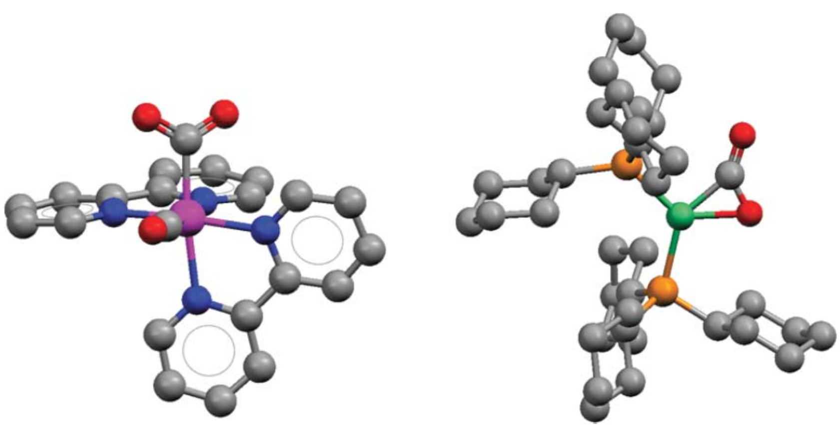

Fig. 7 Structural representations of the bent η^1-**C**O$_2$ (left, [(bpy)$_2$Ru(CO_2)(CO)]) and η^2-**OC**O (right, [(Cy$_3$P)$_2$Ni(CO_2)]) coordination modes (CCDC codes: VUDKIO (left), DAJCUM (right)).

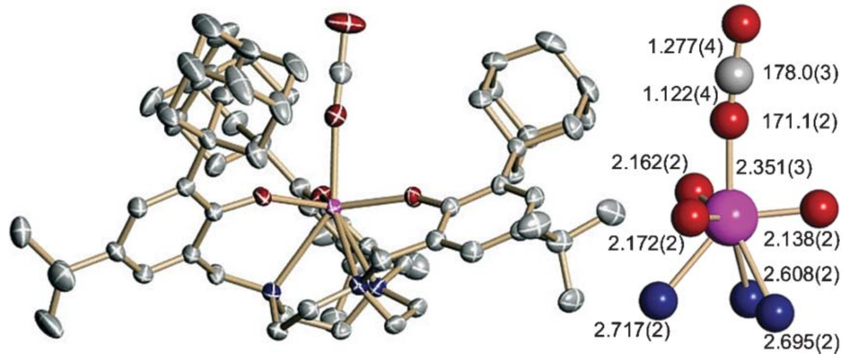

Fig. 8 Molecular representation of $[((^{Ad}ArO)_3tacn)U(CO_2)]$ (**7**, left) with core structure and geometrical parameters (right) in Å and degrees.

reduced by one electron. This reduction results in activation of the inert C=O double-bond and is expected to increase reactivity of the thermodynamically stable CO_2 molecule.

The discrepancy between the significant degree of activation (as judged from the bond distances) and the relatively small red-shift of ν_{as}(OCO) is currently the subject of a computational study.

3. Nitrogen atom transfer chemistry employing uranium complexes

Nitrogen atom transfer chemistry is of considerable interest to inorganic[47,48] and organic[49–53] chemists. While inorganic coordination chemists are fascinated by the reactivity of terminal nitrido ligands,[54] organic chemists employ these reagents for the synthesis of aziridines, highly strained three-membered rings systems that undergo ring-opening to yield the corresponding amino functionality.[53,55] The formal metal-nitrido triple-bond is one of the strongest metal–ligand interactions known to coordination chemists[56,57] and yet, these species can undergo facile and complete inter-metal $2e^-$ and $3e^-$ nitrogen atom transfer reactions.[58] However, for aziridination, the insertion of the nitrido nitrogen into C=C double-bonds, nitrido ligand activation (*e.g.* with TFAA) is often indispensable due to the highly covalent character of the dπ–pπ interaction.[59,60] In contrast, the valence f-orbitals of uranium complexes do not participate in strong covalent bonding. As a result, the uranium–nitrogen moiety is more ionic $U(\delta^+)$–$N(\delta^-)$ and thus, we expected uranium imido and nitrido complexes to be more reactive toward electrophilic substrates.

The enhanced reactivity of **1** and **1-Ad** was ample impetus for us to explore the synthesis of high-valent uranium imido and nitrido complexes and probe them for their application in nitrogen atom- and group transfer chemistry.

In our attempts to synthesize high-valent uranium complexes with multiple-bonded N ligands, the trivalent uranium starting complexes **1** and **1-Ad** were treated with various organic azides following reported protocols. We found that reaction of **1** with one equivalent of trimethylsilyl azide in hexane yielded the expected uranium(V) imido $[((^{t\text{-}Bu}ArO)_3tacn)U(NSiMe_3)]$ (**8**) as well as a uranium(IV) azido species $[((^{t\text{-}Bu}ArO)_3tacn)U(N_3)]$ (**9**).[27] Reaction of trivalent acetonitrile complex **4** with trimethylsilyl azide yielded complex **9** exclusively. In accordance with literature reports, we suggest that pentavalent complex **8** forms through coordination of the azide's N_α atom (R–N_α–N_β–N_γ), in a second step dinitrogen is expelled, and lastly, the formally electron-deficient trimethylsilyl nitrene oxidizes the trivalent uranium ion by two units to yield a U(V) imido complex. Formation of an azido complex, such as **9**, is without precedent and could be explained by coordination of the azides' terminal N_γ atom with subsequent homolytic Si–N_α bond cleavage that leads to a $Me_3Si^\bullet$ and $N_3^\bullet$ radical. While the $Me_3Si^\bullet$ radical recombines to form Me_6Si_2, the azide radical oxidizes the U(III) complex to form the U(IV) azido complex **9**. Steric considerations in seven-coordinate **4** do not allow for metal-coordination of the crowded N_α azide nitrogen. As a result, coordination of the unhindered terminal N_γ atom is enforced, followed by radical elimination and $1e^-$ oxidation. This suggested mechanism is supported by the U(III)/U(IV) oxidative driving force and would be facilitated by an organic azide that permits homolytic N_α–R bond cleavage.

This hypothesis was tested by employing organic azides with different N_α–C bonds. While trityl azide (Ph_3C–N_3) will readily cleave its C–N_α bond (forming Gomberg's dimer), the homolytic bond cleavage in adamantyl azide (Ad–N_3) is energetically not favorable; formation of the U(V) imido species should thus be preferred. As shown in Scheme 5, compound **9** can be obtained reproducibly by treating **1** with trityl azide. In addition, the imido species $[((^{t\text{-}Bu}ArO)_3tacn)U(N(CPh_3))]$ (**8b**) is formed in 40% yield as a by-product.

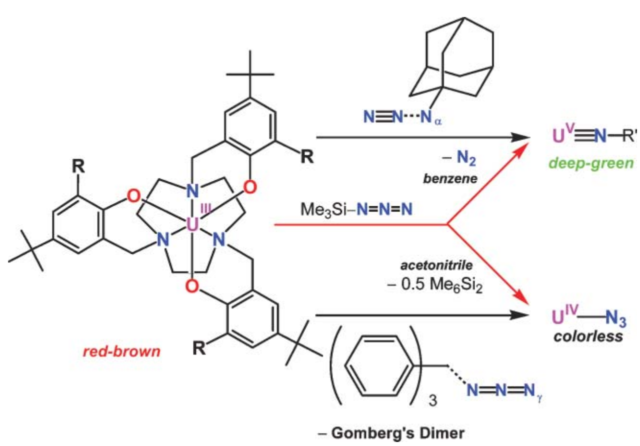

Scheme 5 Reaction of trivalent **1** (R = t-Bu) and **1-Ad** (R = Ad) with various organic azides.

Table 2 Selected structural parameters for complexes [((${}^{t\text{-}Bu}$ArO)$_3$-tacn)U(NSiMe$_3$)] (**8**, two independent molecules), [((${}^{t\text{-}Bu}$ArO)$_3$-tacn)U(N$_3$)] (**9**), [((^{Ad}ArO)$_3$tacn)U(N$_3$)] (**10**), and [((^{Ad}ArO)$_3$-tacn)U(NSiMe$_3$)] (**11**), (Bond distances in Å, bond angles in °)

Structural parameters	8	11	9	10
d(U–N1$_{tacn}$)	2.719(5)/2.791(4)	2.675(2)	2.825(9)	2.667(3)
d(U–N2$_{tacn}$)	2.737(5)/2.724(4)	2.729(2)	2.758(9)	2.661(3)
d(U–N3$_{tacn}$)	2.660(5)/2.735(4)	2.683(2)	2.886(9)	2.649(3)
d(U–N$_{av}$)	2.70/2.75	2.70	2.83	2.66
d(U–O1$_{ArO}$)	2.196(4)/2.161(4)	2.2028(17)	2.294(8)	2.171(2)
d(U–O2$_{ArO}$)	2.203(4)/2.185(4)	2.2179(17)	2.295(8)	2.152(2)
d(U–O3$_{ArO}$)	2.209(4)/2.222(4)	2.2109(17)	2.286(8)	2.143(2)
d(U–O$_{av}$)	2.20/2.19	2.21	2.29	2.16
d(U–N$_{azido}$)	—	—	2.564(12)	2.372(3)
d(U–N$_{imido}$)	1.985(5)/1.992(4)	2.1219(18)	—	—
U$_{out\text{-}of\text{-}plane\ shift}$	0.151	0.188	0.308	0.292
∠(U–N$_{imido}$–Si)	178.5(3)/168.9(3)	162.55(12)	—	—
∠(U–N$_\alpha$–N$_\beta$)	—	—	145.6(9)	176.9(8)

In contrast, treatment of **1** with 1-adamantyl azide produces the uranium(V) imido species [((${}^{t\text{-}Bu}$ArO)$_3$tacn)U(N(Ad))] (**8c**), exclusively.[27]

Like transition metal imido complexes, high-valent uranium(V) and (VI) imido species typically exhibit short, formal U≡N(imido) triple bonds with bond distances ranging from 1.85 to 2.01 Å and ∠(U–N–R) bond angles varying from slightly bent to linear (163.33–180.0°).[27,61–68] Accordingly, the structural parameters of imido complexes **8** and **8b** (d(U–N(imido)) = 1.989(5) and 1.992(4) Å and ∠(U–N–R) = 173.7(3) and 177.7(3)°) are similar to those reported for other metal imido complexes in the literature.[27] As a result of strong bonding to the axial imido ligand, the U ion in **8** and **8b** moves closer to the trigonal plane formed by the three aryloxide oxygens and is found to be −0.151 (**8**) and −0.148 Å (**8b**) below the plane.

In contrast to the large number of transition metal azido complexes, only few uranium azido species have been reported in the literature.[69,70] The molecular structure of the uranium(IV) azide complex in crystals of **9** resembles those of typical metal azido complexes. The linear N$_3^-$ ligand (∠N$_\alpha$–N$_\beta$–N$_\gamma$ = 178.2(14)°) is bound to the metal ion in a bent fashion with an U–N$_\alpha$–N$_\beta$ angle of 145.9(9)°. The uranium–azide bond distance was determined to be 2.564(12) Å and the weakly bound azide ligand in **9** leads to an average out-of-plane shift of the uranium(IV) ion of −0.307 Å.

Neither of the above described azido and imido uranium complexes [((${}^{t\text{-}Bu}$ArO)$_3$tacn)U(L)] (L = N$_3^-$ (**9**) and RN^{2-} (R = SiMe$_3$ (**8**), CPh$_3$ (**8b**))),[27] however, could be transformed to a high-valent uranium nitrido species (*via* thermolysis, photolysis or Si–N bond cleavage) nor did they exhibit the desired nitrogen atom nucleophilicity and resulting atom and/or group transfer chemistry. However, steric pressure introduced by a bulkier chelator was expected to increase the complexes' reactivity. Accordingly, the sterically encumbering [((^{Ad}ArO)$_3$tacn)U] (**1-Ad**) was employed in the reaction with organic azides.

3.1 Reactivity induced by steric pressure in [((^{Ad}ArO)$_3$tacn)U(L)] complexes

Similar to **1**, complex **1-Ad** reacts with one equivalent of trimethylsilyl azide to yield the uranium(IV) azido complex [((^{Ad}ArO)$_3$tacn)U(N$_3$)] (**10**, *via* Me$_3$Si radical elimination and formation of Me$_6$Si$_2$) and the uranium(V) imido species [((^{Ad}ArO)$_3$tacn)U(NSiMe$_3$)] (**11**, with evolution of N$_2$).[71]

The X-ray diffraction analysis of **10** and **11** clearly demonstrated the influence of the sterically more demanding adamantyl groups in these complexes. A comparison of selected structural parameters found in complexes of **10** and **11** with those in the sterically unhindered **8** and **9** is given in Table 2; structural representations of imido complexes **8** and **11** are depicted in Fig. 9. The most remarkable difference between azido complexes **9** and **10** is the linearly coordinated azido ligand in **10** (∠(U–N$_\alpha$–N$_\beta$) = 145.6(9)° (**9**) *vs.* ∠(U–N$_\alpha$–N$_\beta$) = 175.6(3)° (**10**)). This linear coordination leads to an increased M–L orbital overlap, resulting in significantly shorter U–N$_3$ bond distances d(U–N$_3$) = 2.564 (**9**) *vs.* 2. 372(3) Å (**10**).

The structural parameters of imido complex **8** are also strongly affected by the adamantyl-derivatized ligand. The U–N(imido) bond distance found in **11** is the longest ever reported for a metal imido complex and deviates significantly from linearity (d(U–N(imido)) = 2.1219(18) Å and ∠(U–N–R) = 162.55(12)°). Additionally, the out-of-plane shift in **11** was found to be −0.188 Å in comparison to −0.151 and −0.148 Å

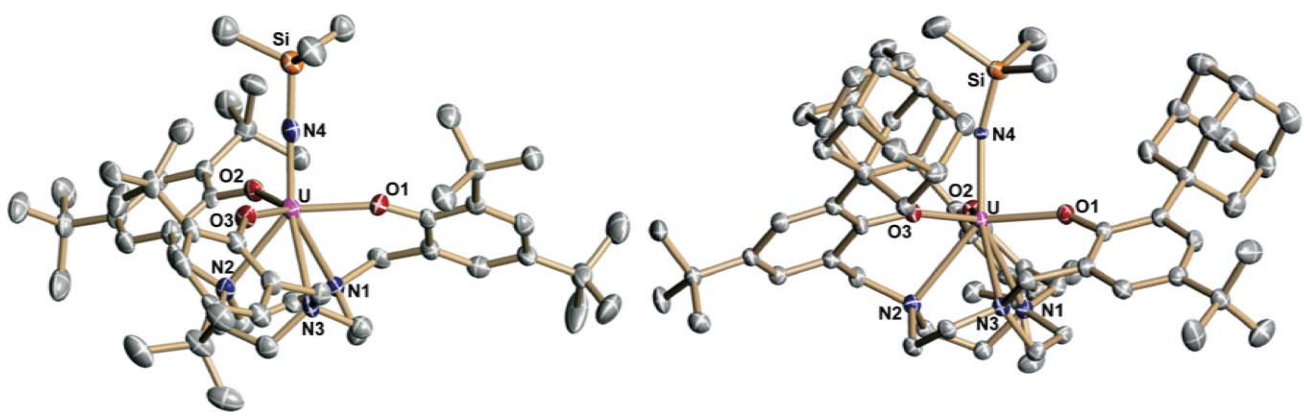

Fig. 9 Comparison of molecular structures of [((^{R}ArO)$_3$tacn)U(NSiMe$_3$)] with R = t-Bu (**8**, left) and Ad (**11**, right).

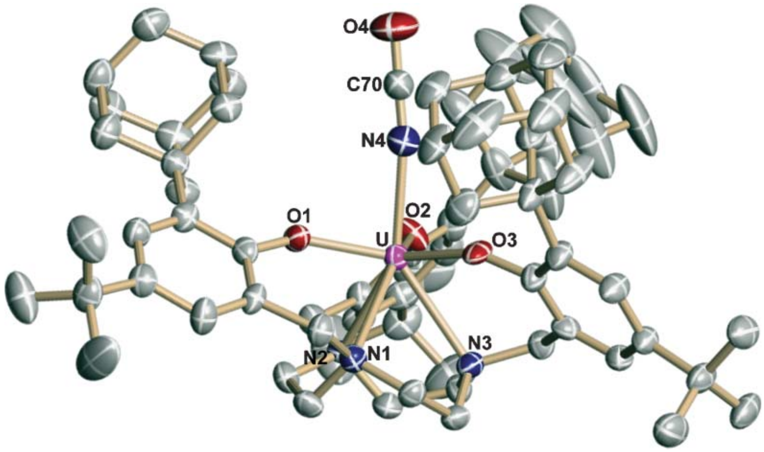

Fig. 10 Molecular representation of [((^{Ad}ArO)$_3$tacn)U(NCO)] (**12**).

in sterically unhindered **8** and **8b**, respectively. These unusual structural features of **11** are likely due to the steric pressure brought about by the sterically encumbering adamantane groups that form a narrow cylindrical cavity and prevent the Me_3SiN^{2-} from optimal binding. Accordingly, the imido nitrogen p-orbitals cannot participate in efficient M–L π-bonding, which results in the observed structural parameters of **11**.

It is expected that the peculiar structural features observed in complexes **10** and **11** (compared to **8** and **9** as well as other known azido and imido species) will result in an increased and atypical reactivity of the axial ligand.

3.2 Nitrogen atom transfer *via* multiple bond metathesis

While imido complex **8** was unreactive towards π-acids, we found that complex **11** reacts cleanly with CO (1 atm) and CH_3NC (1 eq.) to form the uranium(IV) isocyanate complex [((^{Ad}ArO)$_3$tacn)U(NCO)] (**12**) and carbodiimide complex [((^{Ad}ArO)$_3$tacn)U(NCNMe)] (**13**) with concomitant formation of $Me_3Si^{\bullet}$ which immediately recombines to produce Me_6Si_2.[71] The IR spectra of **12** and **13** exhibit one strong vibrational band centered at 2185 and 2101 cm^{-1} that can be assigned to the η^1-coordinate isocyanate (**12**) and carbodiimide (**13**) ligands. Elemental analysis (C, H, N) and ^{1}H NMR spectroscopy suggest that complexes **12** and **13** are isoelectronic and isostructural to the previously prepared uranium(IV) heterocumulene complexes [((^{Ad}ArO)$_3$tacn)U(η^1-OCO)] (**7**) and [((^{Ad}ArO)$_3$tacn)U(η^1-N$_3$)] (**10**).[37]

The X-ray crystallographic analysis of **12** and **13** confirmed formation of nearly linear, axial η^1-bound isocyanate and carbodiimide ligands in these complexes (Fig. 10 and 11). The U–N4 bond distances and ∠(U–N4–C70) angles were determined to be 2.389(6) Å and 171.2(6)° in **12** and 2.327(3) Å and 161.9(3)° in **13** and are very similar to the corresponding parameters found in **7** and **10**. Likewise, the inner N–C–O and N–C–NMe angles of 178.2(9)° and 174.3(4)°, respectively, are also close to linear. The out-of-plane shifts of the uranium ion with respect to the tris-aryloxide plane are −0.301 and −0.318 Å for **12** and **13**. As mentioned earlier, these out-of-plane shifts are generally very sensitive to the formal oxidation state of the uranium center. The shifts of the central U ion of complexes **12** and **13** fall between the values found for the analogous U(V) and U(III) complexes and therefore appear to indicate a formal U(IV) oxidation state for **12** and **13**.

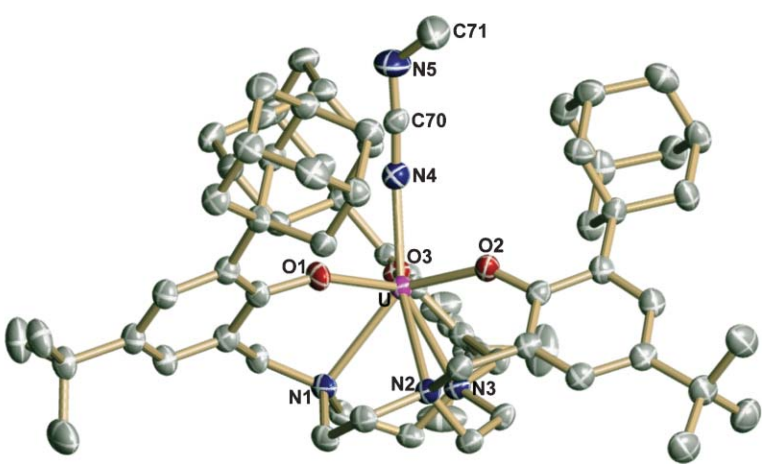

Fig. 11 Molecular representation of [((^{Ad}ArO)$_3$tacn)U(NCNCH$_3$)] (**13**).

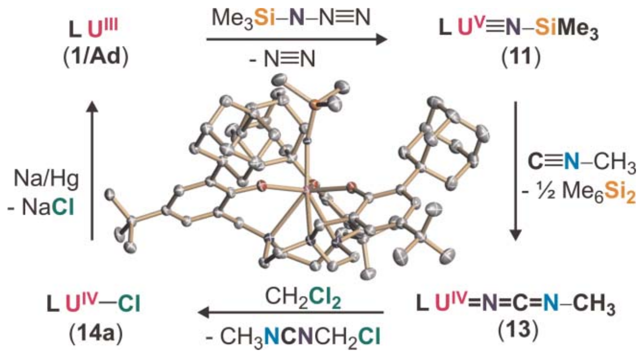

Scheme 6 Synthesis of complexes and nitrogen-atom transfer chemistry in successive one-electron steps.

Interestingly, the isocyanate and carbodiimide ligands of **12** and **13** are reactive and can be transferred to organic molecules. For instance, the carbodiimide ligand in **13** reacts with CH_3I or CH_2Cl_2 to release the functionalized organic carbodiimides, CH_3NCNCH_2Cl and CH_3NCNCH_3, yielding the corresponding halide complexes $[((^{Ad}ArO)_3tacn)U(X)]$ (X = Cl (**14a**), I (**14b**); Scheme 6, **11** → **14a**).[71] Furthermore, these halide complexes can be regenerated to the uranium(III) starting complex **1-Ad** *via* sodium/amalgam reduction. This series of reactions represents a synthetic cycle **1-Ad** → **11**→ **13** → **14a** → **1-Ad**, in which the imido nitrogen atom (or intermediate *nitrido* nitrogen) is transferred from the uranium complex and incorporated into an organic substrate *via* C≡O and R′N≡C/U≡NR multiple-bond metathesis in successive one-electron events. A close examination of the calculated frontier orbitals in **11** suggests that the remarkable reactivity of the uranium imido complex **11** originates from a high degree of ionic character within the U^{5+}–NR^{2-} moiety. This bond is very different from imido and nitrido bonds of group 6 transition metal complexes, which typically exhibit very strong covalent multiple bonds.

4. Electronic structure of low and high-valent uranium complexes

In contrast to light transition metal complexes, magnetic susceptibility data for actinide complexes do not allow for simple interpretations and thus, do not provide instant information on the number of unpaired electrons and the complexes' formal oxidation state. Due to large spin–orbit coupling constants (ξ) and relatively small interelectronic repulsion interactions (e^2/r) in addition to electric field terms (V) that often are comparable in magnitude to ξ and e^2/r, the Russell–Saunders (L–S) coupling formalism cannot be applied nor can it be replaced by *jj*-coupling.[72] Consequently, relatively few magnetic studies of actinide coordination compounds are reported in the literature,[73] barring the mere report of room-temperature magnetic moments as determined by the Evans' method. Despite these difficulties, we believe that the quantitative comparison of temperature-dependent magnetization data of a series of complexes can provide valuable information. The following is a descriptive chapter, a collection of data rather than a magnetization study on a microscopic level, which is under way and will be reported on in due course. Regardless, the complexes presented above provide a unique opportunity to study the electronic properties of a series of $[((^{R}ArO)_3tacn)U(L)]$ uranium coordination complexes in which the $[((^{R}ArO)_3tacn)U]$–core structure remains unperturbed while the axial ligand L (CH_3CN, N_3^-, OCN^-, CH_3NCN^-, $CO_2^{\bullet-}$, RN^{2-}) varies with the complexes' formal oxidation state (+III to +VI).

The magnetic moments, μ_{eff}, of solid samples of trivalent **1**, **1-Ad**, and **4** are strongly temperature dependent, varying from 1.77, 1.74 and 1.66 μ_B at 5 K to 2.92, 2.83 and 2.90 μ_B at 300 K, respectively (Fig. 12, right). The experimentally determined effective magnetic moments μ_{eff} at room temperature are considerably lower than that calculated for a mononuclear f^3 uranium species with a $^4I_{9/2}$ ground state. The theoretical magnetic moment for an ion with an $5f^3$ configuration is calculated to be $\mu_{eff(calcd)} = g_J(J(J+1))^{1/2} = 3.69\ \mu_B$.[74] The observed reduced magnetic moments of **1-Ad** and **4** are likely due to the strong ligand field, introduced by the equatorial aryloxide oxygen ligands, which splits the $J = 9/2$ ground state in U(III) ions. It is suggested that the splitting of the lowest J manifold is such that the all of the J_z states are not equally populated at room temperature. Consequently, the experimentally observed moments are smaller than the free-ion moment. Minor covalent contributions in U(III) complexes **1** and **4** may further reduce the observed magnetic moment *via* orbital

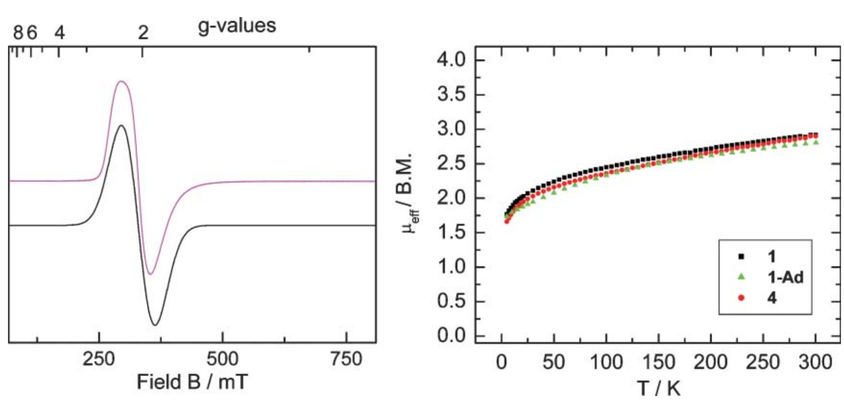

Fig. 12 X-band EPR spectrum of **1-Ad** (left) recorded in frozen benzene solution at T = 14 K. Experimental spectrum (magenta): frequency, 9.4666 GHz; power, 0.63 mW; modulation amplitude, 10 G. Simulation (in black): g = 2.005, W_{FWHM} = 400 G and temperature dependent SQUID magnetization data for **1**, **1-Ad**, and **4** (right).

reduction. In contrast, the experimentally determined magnetic moments of U(IV) (f^2) complexes at room temperature are generally similar but, surprisingly, sometimes even higher ($\mu_{eff(expt)} \approx$ 3–3.5 μ_B) than the analogous moments of the U(III) f^3 ions of the [((^RArO)$_3$tacn)U(L)]-system.

Note that the theoretically expected moment 3.58 μ_B for a U(IV) ion with an f^2 electron configuration and $^3H_4$ ground state is only $\sim$0.1 μ_B lower than 3.69 μ_B expected for an U(III) ion with three unpaired f-electrons.

Accordingly, room-temperature magnetic moments often do not permit for an unambiguous assignment of the +3 and +4 oxidation state in molecular uranium compounds.[73] However, the temperature dependence of μ_{eff} in the range 4–300 K and especially the low-temperature behavior below 75 K, often allows for a clear assignment of U(III) and U(IV) oxidation states. Generally U(IV) complexes possess a singlet ground state that exhibits temperature-independent paramagnetism (TIP) at low temperatures, resulting in magnetic moments of *ca.* 0.5–0.8 μ_B at approx. 4 K (Fig. 13).[73]

In contrast, an isolated f^3 ion cannot be an orbital singlet and thus, the doublet ground state in mononuclear trivalent uranium complexes gives rise to higher magnetic moments at low temperature; in case of **1**, **1-Ad**, and **4**, moments of $\sim$1.7 μ_B are observed at 4 K. Notably, we found that frozen solutions of trivalent uranium complexes **1-Ad**, **4**, and [U(N(SiMe$_3$)$_2$)$_3$] are EPR active at temperatures below 20 K. X-band EPR spectra of **4** and [U(N(SiMe$_3$)$_2$)$_3$] show broad and unsymmetrical signals centered at g = 2.016 and 2.50, respectively. The spectrum of **1-Ad**, recorded in frozen benzene solution at 14 K, exhibits a metal-centered isotropic signal at g = 2.005 (Fig. 12, left), which is in excellent agreement with its low-temperature magnetic moment of μ_{eff} = 1.73μ_B = ½$(3g^2)^{1/2}$.

Despite the difficulties in understanding the magnetism of complexed actinide ions, the most remarkable spectroscopic difference between trivalent and tetravalent uranium complexes of the [((^RArO)$_3$tacn)U(L)]-type is their characteristic color. In contrast to their deeply colored red–brown to purple trivalent analogues, uranium(IV) complexes appear very pale aquamarine/blue–green in the solid state and almost colorless in solution. Accordingly, electronic absorption spectra of all U(IV) complexes [((^RArO)$_3$tacn)U^{IV}(L)] show very similar spectra with various sharp, low intensity bands (ε = 5–80 M^{-1} cm^{-1}) between 350–2100 nm. These bands originate from Laporte-forbidden f–f transitions. In addition to these characteristic low-intensity f–f transitions in the visible and near-infrared region between 500 and 2200 nm, U(III) complexes often show intense, color-giving d–f transitions in the visible part of the absorption spectrum.[75]

The temperature dependence of μ_B of molecular complexes of uranium(V) (f^1) is clearly distinguishable from their f^2 and f^3 analogues. For example, derivatives of pentavalent imido complexes **8** and **11** show temperature-dependent magnetic moments that vary from $\sim$1.5 μ_B at 5 K to $\sim$2–2.4 μ_B at 300 K (Fig. 14). These observed moments are reduced significantly below the theoretical value of 2.54 μ_B, calculated for a free ion in the *L–S* coupling scheme,[72] and are always lower than their corresponding f^2 and f^3 counterparts in the [((^RArO)$_3$tacn)U(L)]-system. Boudreaux and Mulay[72] have attributed this phenomenon to covalency effects in high-valent uranium complexes, in which the high-oxidation state is often stabilized by strongly π-donating ligands, such as terminal oxo or, as in **8** and **11**, strongly bound imido ligands. In both cases, the metal–ligand interactions can be best described as formal M≡L triple bonds.

Like the trivalent complexes with the (^RArO)$_3$tacn ligand, the uranium(V) imido species of this ligand system are intensely colored. Derivatives of **8** and complex **11** are deep-green in color and show intense ligand-to-metal charge-transfer bands below 500 nm. In addition, their spectra also show numerous weak but sharp absorption bands in the visible and near infrared region between 500 and 2200 nm (ε = 20–100 $M^{-1}cm^{-1}$), characteristic for f–f transitions.

5. Is the CO_2 ligand in [((^AdArO)$_3$tacn)U(CO_2)] activated?

The large number of isostructural and isoelectronic complexes that have been obtained allows for a systematic study of their

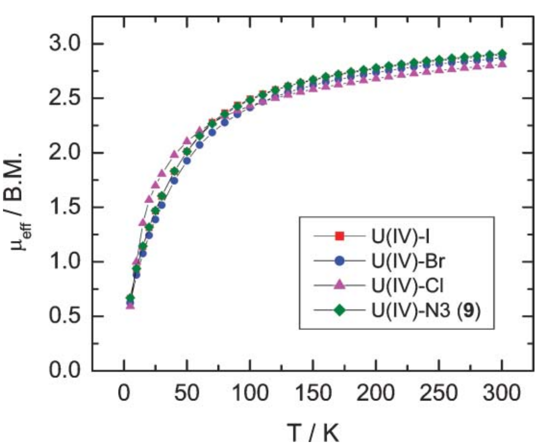

Fig. 13 Temperature-dependent SQUID magnetization data for [((^AdArO)$_3$tacn)U(N_3)] (**9**) and closely related U(IV) halide complexes [((^AdArO)$_3$tacn)U(Cl)], [((^AdArO)$_3$tacn)U(Br)], and [((^AdArO)$_3$tacn)U(I)].

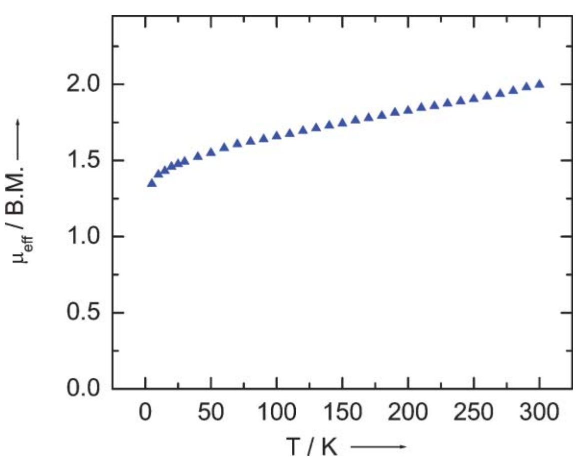

Fig. 14 Temperature dependent SQUID magnetization data for the U(V) complex [((^AdArO)$_3$tacn)U(NSi(CH_3)$_3$)] (**11**).

Oxidation-state	oop-Shift (in Å)	Complex (L_{ax})	
3	– 0.442	**4**	CH_3CN
3.5	– 0.377	**5**	μ–CO
3.5	– 0.368	**6**	μ–N_3
4	– 0.308	**7**	OCO
4	– 0.318	**9**	N_3
4	– 0.290	**14**	Cl
4	– 0.301	**12**	NCO
4	– 0.318	**13**	NCNMe
4	– 0.292	**10**	N_3
5	– 0.151	**8**	NSiMe
5	– 0.147	**8b**	$NCPh_3$
5	– 0.188	**11**	NSiMe

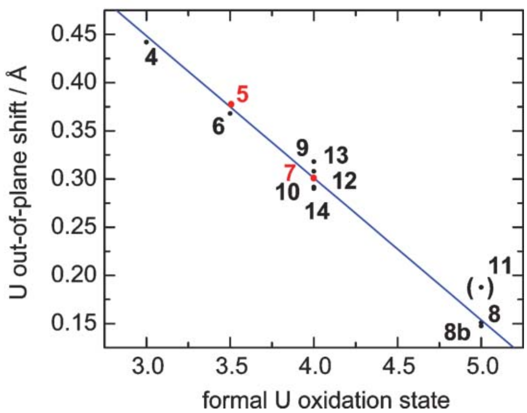

Fig. 15 Summary of out-of-plane shifts *vs.* oxidation state for complexes $[((^{R}ArO)_3tacn)U(L_{ax})]$.

molecular and electronic structures. It is interesting to compare structural and spectroscopic features of the fascinating and unique U–CO_2 complex (**7**) to analogous complexes. In the following section, we will compare **7** to the series of complexes $[((^{Ad}ArO)_3tacn)U^{n}(L)]^{m+}$ (n = III, IV, V, VI; m = 0, 1; and L = CH_3CN, N_3^-, CH_3NCN^-, OCN^-, and RN^{2-}) and discuss whether or not the bound CO_2 ligand in $[((^{Ad}ArO)_3tacn)U(CO_2)]$ is "activated" or "reduced" and if so, to what degree.

A coordination chemist is trained to observe color changes during the course of a chemical reaction. While this certainly is by no means "high-tech", it is worth mentioning that the chemist who synthesized the colorless $[((^{Ad}ArO)_3tacn)U(CO_2)]$ immediately "knew" that the deeply-colored trivalent starting complex $[((^{Ad}ArO)_3tacn)U]$ was oxidized to uranium(IV) upon reaction with CO_2. Why? Because of the observed color change! It was emphasized earlier that, while U(III) and U(V) complexes are red and green colored, respectively, all U(IV) complexes $[((^{Ad}ArO)_3tacn)U^{IV}(L)]$ are colorless. Exposure of toluene solutions or even solid samples of deeply red-colored **1-Ad** to CO_2 gas resulted in instantaneous discoloration and, eventually, colorless crystals were obtained. Its solution UV/vis/NIR electronic absorption spectrum is strikingly similar to all other U(IV) complexes synthesized in this study. All other spectroscopic evidence, including advanced techniques, such as single-crystal diffraction, X-ray absorption and SQUID magnetization studies, as well as the standard laboratory spectroscopy techniques that were accumulated so far suggest that the U ion in **7** is oxidized by $1e^-$ and thus, the CO_2 ligand is reduced to a $CO_2^{-\bullet}$ radical anion.

The molecular structure of **7** already revealed bond distances of the coordinated CO_2 ligand that were quite different from those of the symmetrical free CO_2 and thus, suggested a significant degree of ligand reduction. The uranium ion's displacement from the idealized trigonal plane of the three aryloxide ligators further implies the U ions' oxidation upon CO_2 binding. While the out-of-plane shift in precursor **1-Ad** was determined to be −0.88 Å, the U ion in **7** and *all other* U(IV) heterocumulene complexes of the $[((^{Ad}ArO)_3tacn)U^{IV}(L)]$ system is displaced only 0.29–0.32 Å below the plane (Fig. 15). In fact, an extrapolation of all available out-of-plane shifts *vs.* oxidation state places the two complexes with ambiguous oxidation states, $[((^{Ad}ArO)_3tacn)U(CO_2)]$ and $[\{((^{t\text{-}Bu}ArO)_3tacn)U\}_2(\mu\text{-}CO)]$, correctly at +4 and +3.5.

Spectroscopic data further support an intramolecular redox-reaction upon CO_2 coordination to **1-Ad**. The vibrational spectrum of **7** exhibits a band at 2188 cm^{-1} that shifts to 2128 cm^{-1} upon ^{13}C isotope labeling. Although this band can be assigned unambiguously to the asymmetric stretching vibration of the coordinated CO_2 ligand, a significantly higher red-shift is expected for a $1e^-$ reduced CO_2 ligand. Accordingly, upon initial observation, a comparison of CO_2 stretching frequencies to those of known M−CO_2 complexes, which feature signals $\nu(CO_2)$ between 1600 and 1750 cm^{-1}, suggests that the activation found in **7** cannot be a "complete" one-electron reduction. However, considering the linear η^1-OCO coordination mode in **7**, which is unprecedented, a comparison of vibrational frequencies with complexes that possess bent C-bound (η^1-**C**OO) or C,O-bound (η^2-**OC**O) CO_2 ligands may not be valid.

SQUID magnetization measurements of **7** were recorded and compared to the large number of similar complexes (Fig. 16). The magnetic moment μ_{eff} of **7** was determined to be 2.89 μ_B at 300 K and 1.51 μ_B at 5 K. Although the

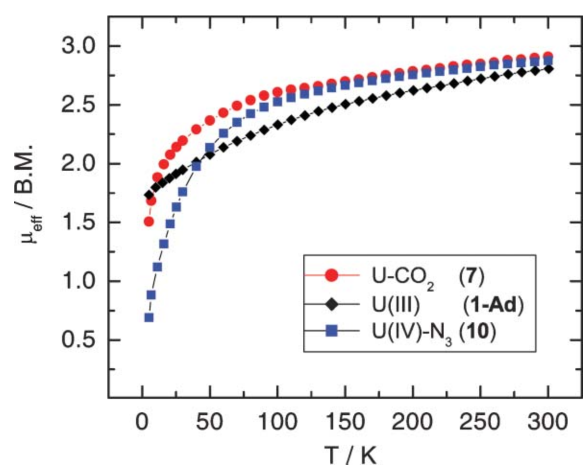

Fig. 16 Temperature dependent SQUID magnetization data for the U(III) and U(IV) complexes $[((^{Ad}ArO)_3tacn)U]$ (**1-Ad**), $[((^{Ad}ArO)_3tacn)U(N_3)]$ (**9**), and $[((^{Ad}ArO)_3tacn)U(CO_2)]$ (**7**).

room-temperature moment of **7** is close to the magnetic moment found for the azide complex **10**, the low-temperature value is similar to that of the U(III) (f^3) starting material **1-Ad** (1.73 μ_B at 5 K), which has a doublet ground state at low temperatures. As mentioned above, the magnetic moments of U(III) (f^3) and U(IV) (f^2) complexes at room temperature are generally very similar and often do not allow for an unambiguous assignment of the complexes' oxidation state. The temperature dependence of μ_B in the range 4–300 K, however, shows a curvature reminiscent of data obtained for all closely-related U(IV) complexes of this type. Although U(IV) complexes possess a singlet ground state, which typically results in magnetic moments of *ca.* 0.5–0.8 μ_B, the magnetic moment of **7** at low temperatures is significantly higher, suggesting that the open-shell $CO_2^{\cdot -}$, unlike the closed-shell N_3^- ligand, likely contributes to the observed increased magnetic moment of **7** at low temperatures. The temperature dependence and low temperature value of **7** are in agreement with the description of the CO_2 ligand as a one-electron reduced $CO_2^{\cdot -}$ radical anion coordinated to a U(IV) ion.

Finally, in order to unambiguously determine the uranium ion's +IV oxidation state in **7**, UL_3 edge energy XANES measurements of the isostructural complexes $[((^{Ad}ArO)_3\text{-tacn})U^m(L)]^{n+}$ (with L = CH_3CN, N_3^-, and Me_3SiN^{2-}, m = III, IV, V, and VI, and $n = 0,1$) were performed and compared to **7**. Details of this study will be published elsewhere. However, preliminary data analysis shows the UL_3 edge energy for $[((^{Ad}ArO)_3tacn)U(CO_2)]$ is virtually identical to that measured for the uranium IV complex $[((^{Ad}ArO)_3tacn)U(N_3)]$. This observation confirms the +IV oxidation state in $[((^{Ad}ArO)_3tacn)U^{IV}(\eta^1\text{-}CO_2^{\cdot -})]$, which implies that the coordinated carbon dioxide ligand is in fact reduced by one electron. Future computational studies will attempt to shed light on the peculiar electronic structure and spectroscopic features, such as the complexes relatively low $\nu_{as}(CO_2)$ red-shift.

5. Concluding remarks

Our laboratory has shown that an aryloxide-functionalized triazacyclononane ligand can be an impressive effector for unique binding and small-molecule activation at low-valent uranium centers, resulting in potentially effective agents for functionalization of otherwise inert molecules. The series of complexes described herein are distinctive in the respect that they represent a set of isostructural complexes possessing a range of oxidation states, as well as differing electronic and magnetic behaviors. This presents a distinct benefit for the understanding of fundamental actinide chemistry in general and uranium in particular. Topics such as the nature of covalency and the role of f-orbitals in bonding can be advanced. After several years of uranium research we are still very excited about this unique class of actinide compounds and are certain that more unexpected and novel reactivity is still to be discovered in the future.

Acknowledgements

This research was supported by the U.S. Department of Energy (DE–FG02-04ER15537), the Alfred P. Sloan Foundation (fellowship to K.M.), and an ACS-PRF Type G grant (40019-G3). We thank NIH for a fellowship to I.C.-R. (3 T32 DK07233-2651) and Drs Hidetaka Nakai (synthesis, UCSD), Kristian Olsen and Xile Hu (computation, UCSD) as well as Dr Wayne Lukens (electronic structure, Lawrence Berkeley National Laboratory) and Drs Steven Conradson and David Clark (XANES, Los Alamos National Laboratory) for their contributions to this article. We wish to thank Ryan L. Holland and Oanh P. Lam (UCSD) for their assistance in finalizing this manuscript (O. P. L.) and prepaing the cover picture (R. L. H.).

References

1 D. Seyferth, *Organometallics*, 2004, **23**, 3562–3583.
2 I. Korobkov and S. Gambarotta, *Prog. Inorg. Chem.*, 2005, **54**, 321–348.
3 W. G. Vandersluys, C. J. Burns, J. C. Huffman and A. P. Sattelberger, *J. Am. Chem. Soc.*, 1988, **110**, 5924–5925.
4 L. R. Avens, D. M. Barnhart, C. J. Burns, S. D. McKee and W. H. Smith, *Inorg. Chem.*, 1994, **33**, 4245–4254.
5 R. A. Andersen, *Inorg. Chem.*, 1979, **18**, 1507–1509.
6 D. L. Clark, A. P. Sattelberger, S. G. Bott and R. N. Vrtis, *Inorg. Chem.*, 1989, **28**, 1771–1773.
7 L. R. Avens, S. G. Bott, D. L. Clark, A. P. Sattelberger, J. G. Watkin and B. D. Zwick, *Inorg. Chem.*, 1994, **33**, 2248–2256.
8 D. L. Clark, A. P. Sattelberger and R. A. Andersen, *Inorg. Synth.*, 1997, **31**, 307–315.
9 J. L. Stewart and R. A. Andersen, *Polyhedron*, 1998, **17**, 953–958.
10 M. Mazzanti, R. L. Wietzke, J. Pecaut, J. M. Latour, P. Maldivi and M. Remy, *Inorg. Chem.*, 2002, **41**, 2389–2399.
11 R. Wietzke, M. Mazzanti, J. M. Latour and J. Pecaut, *J. Chem. Soc., Dalton Trans.*, 1998, 4087–4088.
12 A. J. Amoroso, J. C. Jeffery, P. L. Jones, J. A. McCleverty, L. Rees, A. L. Rheingold, Y. M. Sun, J. Takats, S. Trofimenko, M. D. Ward and G. P. A. Yap, *J. Chem. Soc., Chem. Commun.*, 1995, 1881–1882.
13 P. Roussel, P. B. Hitchcock, N. Tinker and P. Scott, *Chem. Commun.*, 1996, 2053–2054.
14 I. Korobkov, S. Gambarotta, G. P. A. Yap, L. Thompson and P. J. Hay, *Organometallics*, 2001, **20**, 5440–5445.
15 C. C. Cummins, *Prog. Inorg. Chem.*, 1998, **47**, 685–836.
16 A. L. Odom, P. L. Arnold and C. C. Cummins, *J. Am. Chem. Soc.*, 1998, **120**, 5836–5837.
17 P. Roussel and P. Scott, *J. Am. Chem. Soc.*, 1998, **120**, 1070–1071.
18 P. Roussel, R. Boaretto, A. J. Kingsley, N. W. Alcock and P. Scott, *J. Chem. Soc., Dalton Trans.*, 2002, 1423–1428.
19 P. L. Diaconescu, P. L. Arnold, T. A. Baker, D. J. Mindiola and C. C. Cummins, *J. Am. Chem. Soc.*, 2000, **122**, 6108–6109.
20 P. L. Diaconescu and C. C. Cummins, *J. Am. Chem. Soc.*, 2002, **124**, 7660–7661.
21 I. Korobkov, S. Gambarotta and G. P. A. Yap, *Angew. Chem., Int. Ed.*, 2002, **41**, 3433–3436.
22 I. Castro-Rodriguez, K. Olsen, P. Gantzel and K. Meyer, *Chem. Commun.*, 2002, 2764–2765.
23 B. Monteiro, D. Roitershtein, H. Ferreira, J. R. Ascenso, A. M. Martins, A. Domingos and N. Marques, *Inorg. Chem.*, 2003, **42**, 4223–4231.
24 M. Nierlich, J. M. Sabattie, N. Keller, M. Lance and J. D. Vigner, *Acta Crystallogr., Sect. C*, 1994, **C50**, 52–54.
25 P. Chaudhuri and K. Wieghardt, *Prog. Inorg. Chem.*, 2001, **50**, 151–216.
26 H. Nakai, X. Hu, L. N. Zakharov, A. L. Rheingold and K. Meyer, *Inorg. Chem.*, 2004, **43**, 855–857.
27 I. Castro-Rodriguez, K. Olsen, P. Gantzel and K. Meyer, *J. Am. Chem. Soc.*, 2003, **125**, 4565–4571.
28 A. Mendiratta and C. C. Cummins, *Inorg. Chem.*, 2005, **44**, 7319–7321.
29 I. Castro-Rodriguez, H. Nakai, P. Gantzel, L. N. Zakharov, A. L. Rheingold and K. Meyer, *J. Am. Chem. Soc.*, 2003, **125**, 15734–15735.

30 The methyl group, CH_3, as a whole is assigned the van der Waals radius 2.0 Å. According to Pauling, the methylene group, CH_2, can be assigned the same value. The van der Waals radius for uranium was taken as 1.9 Å.
31 L. Pauling, *The Nature of the Chemical Bond*, Cornell University Press, Ithaca, New York, 3rd edn, 1960.
32 J. E. Huheey, E. A. Keiter and R. L. Keiter, *Inorganic Chemistry: Principles of Structure and Reactivity*, HarperCollins, New York, 4th edn, 1993.
33 J. G. Brennan, R. A. Andersen and J. L. Robbins, *J. Am. Chem. Soc.*, 1986, **108**, 335–336.
34 J. Parry, E. Carmona, S. Coles and M. Hursthouse, *J. Am. Chem. Soc.*, 1995, **117**, 2649–2650.
35 W. J. Evans, S. A. Kozimor, G. W. Nyce and J. W. Ziller, *J. Am. Chem. Soc.*, 2003, **125**, 13831–13835.
36 I. Castro-Rodriguez and K. Meyer, *J. Am. Chem. Soc.*, 2005, **127**, 11242–11243.
37 I. Castro-Rodriguez, H. Nakai, L. N. Zakharov, A. L. Rheingold and K. Meyer, *Science*, 2004, **305**, 1757–1759.
38 J. G. Brennan, R. A. Andersen and A. Zalkin, *Inorg. Chem.*, 1986, **25**, 1756–1760.
39 J. G. Brennan, R. A. Andersen and A. Zalkin, *Inorg. Chem.*, 1986, **25**, 1761–1765.
40 D. H. Gibson, *Chem. Rev.*, 1996, **96**, 2063–2095.
41 M. Aresta and C. F. Nobile, *J. Chem. Soc., Dalton Trans.*, 1977, 708–711.
42 M. Aresta, C. F. Nobile, V. G. Albano, E. Forni and M. Manassero, *J. Chem. Soc., Chem. Commun.*, 1975, 636–637.
43 T. Herskovitz, *J. Am. Chem. Soc.*, 1977, **99**, 2391–2392.
44 A. Dohring, P. W. Jolly, C. Kruger and M. J. Romao, *Z.Naturforsch., B*, 1985, **40b**, 484–488.
45 H. Tanaka, H. Nagao, S. M. Peng and K. Tanaka, *Organometallics*, 1992, **11**, 1450–1451.
46 H. J. Lee, M. D. Lloyd, K. Harlos, I. J. Clifton, J. E. Baldwin and C. J. Schofield, *J. Mol. Biol.*, 2001, **308**, 937–948.
47 T. Birk and J. Bendix, *Inorg. Chem.*, 2003, **42**, 7608–7615.
48 J. Bendix, *J. Am. Chem. Soc.*, 2003, **125**, 13348–13349.
49 D. A. Evans, M. M. Faul and M. T. Bilodeau, *J. Org. Chem.*, 1991, **56**, 6744–6746.
50 D. A. Evans, M. M. Faul, M. T. Bilodeau, B. A. Anderson and D. M. Barnes, *J. Am. Chem. Soc.*, 1993, **115**, 5328–5329.
51 Z. Li, K. R. Conser and E. N. Jacobsen, *J. Am. Chem. Soc.*, 1993, **115**, 5326–5327.
52 Z. Li, R. W. Quan and E. N. Jacobsen, *J. Am. Chem. Soc.*, 1995, **117**, 5889–5890.
53 D. E. N. Jacquot, M. Zollinger and T. Lindel, *Angew. Chem., Int. Ed.*, 2005, **44**, 2295–2298.
54 J. K. Brask, V. Dura-Vila, P. L. Diaconescu and C. C. Cummins, *Chem. Commun.*, 2002, 902–903.
55 J. DuBois, C. S. Tomooka, J. Hong and E. M. Carreira, *J. Am. Chem. Soc.*, 1997, **119**, 3179–3180.
56 J. Bendix, R. J. Deeth, T. Weyhermuller, E. Bill and K. Wieghardt, *Inorg. Chem.*, 2000, **39**, 930–938.
57 J. P. F. Cherry, A. R. Johnson, L. M. Baraldo, Y. C. Tsai, C. C. Cummins, S. V. Kryatov, E. V. Rybak-Akimova, K. B. Capps, C. D. Hoff, C. M. Haar and S. P. Nolan, *J. Am. Chem. Soc.*, 2001, **123**, 7271–7286.
58 L. K. Woo, *Chem. Rev.*, 1993, **93**, 1125–1136.
59 J. DuBois, C. S. Tomooka, J. Hong, E. M. Carreira and M. W. Day, *Angew. Chem., Int. Ed.*, 1997, **36**, 1645–1647.
60 J. DuBois, C. S. Tomooka, J. Hong and E. M. Carreira, *Acc. Chem. Res.*, 1997, **30**, 364–372.
61 R. E. Cramer, K. Panchanatheswaran and J. W. Gilje, *Angew. Chem., Int. Ed. Engl.*, 1984, **23**, 912–913.
62 J. G. Brennan and R. A. Andersen, *J. Am. Chem. Soc.*, 1985, **107**, 514–516.
63 A. Zalkin, J. G. Brennan and R. A. Andersen, *Acta Crystallogr., Sect. C*, 1988, **C44**, 1553–1554.
64 C. J. Burns, W. H. Smith, J. C. Huffman and A. P. Sattelberger, *J. Am. Chem. Soc.*, 1990, **112**, 3237–3239.
65 D. S. J. Arney and C. J. Burns, *J. Am. Chem. Soc.*, 1993, **115**, 9840–9841.
66 D. S. J. Arney and C. J. Burns, *J. Am. Chem. Soc.*, 1995, **117**, 9448–9460.
67 B. P. Warner, B. L. Scott and C. J. Burns, *Angew. Chem., Int. Ed.*, 1998, **37**, 959–960.
68 J. L. Kiplinger, D. E. Morris, B. L. Scott and C. J. Burns, *Chem. Commun.*, 2002, 30–31.
69 P. Charpin, M. Lance, M. Nierlich, D. Vigner, J. Livet and C. Musikas, *Acta Crystallogr., Sect. C*, 1986, **C42**, 1691–1694.
70 L. Prasad, E. J. Gabe, B. Glavincevski and S. Brownstein, *Acta Crystallogr., Sect. C*, 1983, **C39**, 181–184.
71 I. Castro-Rodriguez and K. Meyer, *Angew. Chem., Int. Ed.*, 2006, in press.
72 E. A. Boudreaux and L. N. Mulay, *Theory and Applications of Molecular Paramagnetism*, John Wiley & Sons, New York, 1976.
73 J. L. Stewart and R. A. Andersen, *New J. Chem.*, 1995, **19**, 587–595.
74 μ_{eff}(calc) = $g_J J(J + 1)^{1/2}$, with the intermediate-coupling Landé splitting factor for $U^3 + g_J = 0.743$, for $^4I_{9/2}$, J is 9/2. E. R. Jones, M. E. Hendricks, J. A. Stone and D. G. Karraker, *J. Chem. Phys.*, 1974, **60**, 2088.
75 J. Katz, L. R. Morss and G. T. Seaborg, *The Chemistry of the Actinide Elements*, Chapman Hall, New York, 1980.

